

Tip region of the bremsstrahlung spectrum from incident electrons of kinetic energy 50 keV–1.84 MeV*

R. H. Pratt and H. K. Tseng[†]

Department of Physics, University of Pittsburgh, Pittsburgh, Pennsylvania 15260

(Received 17 June 1974; revised manuscript received 6 January 1975)

Numerical calculations for the tip region of the electron bremsstrahlung spectrum are reported for incident electron kinetic energies in the range from 50 keV to 1.84 MeV. The calculations are exact within the framework of a single electron in a screened central potential and are obtained by summing integrals resulting from a partial-wave expansion of the wave functions. Results are compared with previous theoretical calculations and with experiments. For low energies the screening correction to the spectrum is generally not small. We find that for high- Z elements the discrepancies between theory and experiment reported by Starek, Aiginger, and Unfried are due to the use of inaccurate theoretical approximation. For low- Z elements the discrepancy remains.

I. INTRODUCTION

High-resolution experimental studies of the tip region of the electron bremsstrahlung spectrum have recently been reported by Starek, Aiginger, and Unfried¹ (SAU). In this region of the spectrum most of the incident-electron kinetic energy is radiated as photon energy k ; the final-electron kinetic energy approaches zero and the familiar Bethe-Heitler² formula predicts that $k d\sigma/dk$ approaches zero. However, this Born approximation calculation is not valid for a slow final electron, and in fact $k d\sigma/dk$ remains finite as k approaches its maximum value. SAU obtained the photon spectrum in the tip region with 3.34-keV photon energy resolution for electrons of kinetic energy 1.84 MeV incident on targets of Li, Al, Cu, Ag, Au, and Pb. Their results for all Z disagreed with the Bethe-Heitler formula but also were not in good agreement with analytic calculations, due to Fano³ and to Elwert and Haug⁴ (EH), which go beyond Born approximation and predict a finite tip limit. The disagreement with Fano and EH was surprising, at least in low- Z elements for which these calculations were expected to be accurate apart from small screening corrections.

We have recently developed a numerical code for the "exact" calculation of bremsstrahlung cross sections in screened potentials V . For a given choice of relativistic self-consistent atomic potential V , initial and final electron wave functions are obtained in partial-wave series by numerically integrating the radial Dirac equation in the potential V . The matrix element reduces to radial integrals over these radial wave functions, performed numerically and then summed. The various partial-wave series are terminated when the contributions of their final terms to the total matrix element become negligible. Nonrelativistic

approximations are not needed and Coulomb and screening effects are fully included, in contrast to all other types of calculation. We have reported results for spectrum points and angular distributions,⁵ for polarization correlations,⁶ and most recently⁷ for the complete photon energy spectra resulting from 50-keV electrons incident on Al and Au. We wish here to present results obtained with this code pertaining to the tip region of the bremsstrahlung spectrum, using the relativistic self-consistent potential of Kohn and Sham.⁸ We will show that for high- Z elements we agree quite well with SAU, while for low- Z elements we confirm the previous theoretical results, leaving the discrepancy unresolved. We will also note what our numerical results say about the properties of the tip cross sections.

Our predictions for the tip region of the bremsstrahlung spectrum are summarized in Tables I and II and Figs. 1–3. Table I presents data in point Coulomb and Kohn-Sham (KS) screened potentials for various choices of atomic number Z and initial electron kinetic energy T_1 , when the fraction of energy k/T_1 radiated is close to 1, as well as an extrapolation to the limiting case $k/T_1=1$. Bethe-Heitler predictions and certain predictions beyond Born approximation are also shown. Table II summarizes these predictions for the tip limit $k/T_1=1$ and also shows results for this limit which can be obtained from atomic photoeffect cross sections. Our predictions for the photon angular distribution are compared with the SAU experimental data and earlier theoretical results in the figures. The tip-limit Z dependence at 10° for 1.84-MeV electrons is shown in Fig. 1; $k d\sigma/dk d\Omega_k$ near the tip at various angles for 0.500-MeV electrons is shown for Al in Fig. 2 and for Au in Fig. 3. Our moderate agreement with SAU for high- Z elements and our disagreement with SAU for low- Z elements is evident.

TABLE I. Comparisons of the tip (or near tip) bremsstrahlung cross sections (k/Z^2) $d\sigma/dk$ for $Z=3, 4, 13, 47, 79,$ and 82 , $T_1=0.050$ – 1.84 MeV as calculated numerically, from the Born approximation, and as predicted by the EH formula. Symbols Coul and KS refer to point-Coulomb and Kohn-Sham potentials, respectively.

Z	T_1 (MeV)	k/T_1	Born (mb)	Exact (mb)		EH (mb)
				Coul	KS	
3	1.84	0.98	0.5124	0.5753	0.5747	0.5675
		0.99	0.3558		0.4269	0.4204
		≈ 0.9978	0.1635		0.2507	0.2478
		0.999	0.1106		0.2073	0.2052
		1.0	0.0		0.165	0.1640
4	0.500	0.90	1.368		1.550	1.526
		0.96	0.8043		1.010	0.9962
		0.98	0.5550		0.7808	0.7714
		0.99	0.3876		0.6349	0.6291
		1.0	0.0		0.454	0.4522
13	0.050	0.99	3.114		22.92	22.18
		0.995	2.197		22.90	22.13
		1.0	0.0	22.9	22.9	22.07
13	0.500	0.90	1.368	1.99	1.978	1.860
		0.96	0.8043		1.517	1.429
		0.98	0.5550		1.361	1.282
		0.99	0.3876		1.293	1.215
		0.995	0.2724		1.272	1.189
47	1.84	0.98	0.5124		1.540	1.146
		0.99	0.3558		1.475	1.094
		≈ 0.9978	0.1635		1.422	1.054
		1.0	0.0	1.27	1.41	1.044
		0.96	6.315	38.09	32.92	27.24
79	0.050	0.98	4.424	37.88	32.80	27.06
		0.99	3.114		32.75	26.99
		1.0	0.0	37.9	32.8	26.98
79	0.180	0.98	1.237		10.54	6.371
		0.99	0.3558		2.096	1.076
79	0.500	0.90	1.368	5.143	4.856	2.478
		0.96	0.8043		4.512	2.233
		0.98	0.5550		4.398	2.158
		0.99	0.3876	4.610	4.339	2.123
		1.0	0.0	4.56	4.30	2.096
79	1.84	0.98	0.5124		2.170	1.125
		0.99	0.3558		2.096	1.076
		≈ 0.9978	0.1635		2.032	1.039
		1.0	0.0		2.02	1.029
82	$2m_e c^2$ ≈ 1.022	0.975	0.5190	3.060		1.350
		0.99	0.3208	2.968		1.295
		1.0	0.0	2.92		1.262

II. GENERAL THEORETICAL APPROACHES

To understand the significance of our comparisons with earlier theoretical work we begin by briefly reviewing some of the general theoretical approaches to the quantum theory of bremsstrahlung. In all cases one wishes to calculate the matrix element

$$M \propto \int \psi_2^* \vec{D} \cdot \vec{\epsilon}^* e^{-i\vec{k} \cdot \vec{r}} \psi_1 d^3r \quad (1)$$

and then a cross section $\sigma \propto p_2 |M|^2$. Here ψ_1 and ψ_2

are initial and final electron wave functions, solutions of the Schrödinger or Dirac equation in the potential $V(r)$. The radiated photon is characterized by its momentum k and polarization vector $\vec{\epsilon}$; the momentum operator \vec{p} is replaced in the relativistic case by the vector matrix $\vec{\alpha}$.

In most previous theoretical work a point-Coulomb potential $V = -Ze^2/r$ is assumed and analytical results are obtained. In the nonrelativistic case exact point-Coulomb continuum wave functions are available. The basic result is due to Sommerfeld⁹ who also made the dipole approximation $e^{-i\vec{k} \cdot \vec{r}} \sim 1$. (When higher multipoles are important relativistic effects can also be expected to contribute.) In the relativistic case the main result has been the Born-approximation calculation of Bethe and Heitler,² expected to be valid for the point-Coulomb potential for low enough Z and high enough initial and final electron velocities $\beta_1 \equiv v_1/c$, $\beta_2 \equiv v_2/c$ such that $Z\alpha/\beta_1$ and $Z\alpha/\beta_2$ are $\ll 1$. For high- Z elements this requirement can never be well satisfied.

Elwert¹⁰ suggested a modification of the Bethe-Heitler formula which extends its usefulness to lower electron velocities. He obtained the ratio of the Sommerfeld formula to the Bethe-Heitler formula in the nonrelativistic region $T_1 \ll 1$, subject to the further assumption $\nu_2 - \nu_1 \ll 1$, where $\nu = Z\alpha/\beta$, and found that, independent of angle, the ratio was given by the factor (Elwert factor)

$$f_E(\nu_2, \nu_1) = (\nu_2/\nu_1)(1 - e^{-2\pi\nu_1})/(1 - e^{-2\pi\nu_2}). \quad (2)$$

If the Bethe-Heitler formula is multiplied by this factor improved results are obtained even for relativistic T_1 and $\nu_2 - \nu_1$ not small. This can be understood once it is recognized that the Elwert factor is the square of the ratio of the nonrelativistic normalizations N of final and initial electron wave functions: $f_E = |N_2/N_1|^2$. But further, written in these variables it is also the ratio of the relativistic normalizations apart from corrections of order $(Z\alpha)^2$. As we will discuss below, when the final electron is of low energy so that ν_2 is large and Born approximation must fail, the important regions of configuration space for the bremsstrahlung matrix element are at small distances. The main error in the Born-approximation wave function of a slow electron at such distances is the replacement of the normalization factor $N \propto |\nu/(1 - e^{-2\pi\nu})|^{1/2} \sim \nu^{1/2}$ for large ν by the Born-approximation (small- ν) value $N \propto (2\pi^{-1/2})$. The term $|N_2|^2$ in the Elwert factor thus serves to correct this major error of Born approximation in situations where ν_1 is small but ν_2 is not. We can also understand the origin of the term $|N_1|^{-2}$ in the Elwert factor. At the other end of the spectrum, when a very soft photon is radiated and the initial

TABLE II. Comparisons of the tip-bremsstrahlung cross sections $(k/Z^2)d\sigma/dk$ (in mb) for $Z=3-82$, $T_1=0.050-1.84$ MeV obtained in our numerical calculations with the exact point-Coulomb results of Brysk-Zerby-Penny (BZP), the predictions of the EH formula, the results using the photoeffect-tip bremsstrahlung connection, and Born approximation normalized with the Sommerfeld-Elwert factor (SE). Coul stands for point-Coulomb.

Z	T_1 (MeV)	Coul				Photoeffect-tip bremsstrahlung connection (Coul)	This work (KS)
		BZP	EH	This work	SE		
3	1.84	...	0.164	...	0.167	...	0.165
4	0.500	...	0.452	...	0.452	...	0.454
13	0.050	...	22.1	22.9	22.1	23.9	22.9
	0.500	...	1.18	1.27	1.18	1.27	1.27
47	1.84	...	1.04	...	1.13	...	1.41
79	0.050	37	27.0	37.9	28.9	42.0	32.8
	0.180	11.3	6.31	...	6.9	13.2	...
	0.380	5.7	2.74	...	3.02	6.42	...
	0.500	4.6	2.10	4.56	2.33	5.08	4.30
	1.84	...	1.03	...	1.24	...	2.02
82	≈ 1.022	...	1.26	2.92	1.46

and final electrons have nearly the same energy, the low-energy theorem states that the bremsstrahlung cross section is proportional to the cross section for elastic electron scattering. But in the nonrelativistic point-Coulomb case the Born-approximation elastic-scattering cross section is the same as the exact Rutherford cross section.

Thus there should be no correction to Born approximation in this case, and the factor $|N_1|^{-2}$ ensures that $f_E=1$ when $\nu_1 \sim \nu_2$. With these two ideas one can understand the nature and extent of the successes of the Elwert factor.

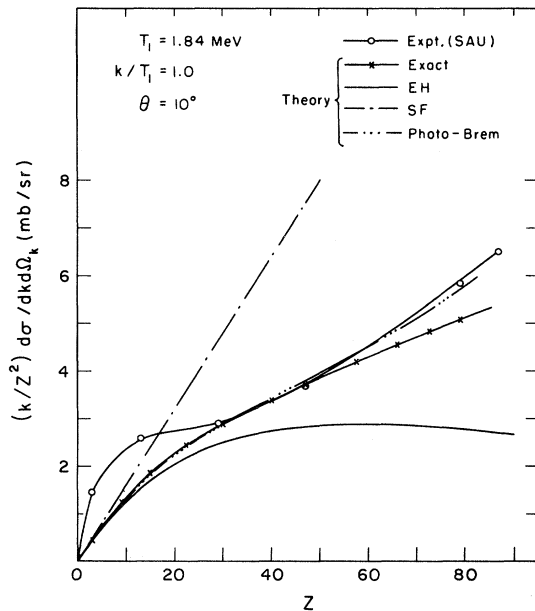


FIG. 1. Comparisons of the bremsstrahlung angular cross section $(k/Z^2) d\sigma/dk d\Omega_k$ at the tip limit for $T_1=1.84$ MeV, $\theta=10^\circ$ between theory and experiment. Note that the EH results given in Fig. 2 of Ref. 1 are incorrect. This error has also been pointed out by the Würzburg group.

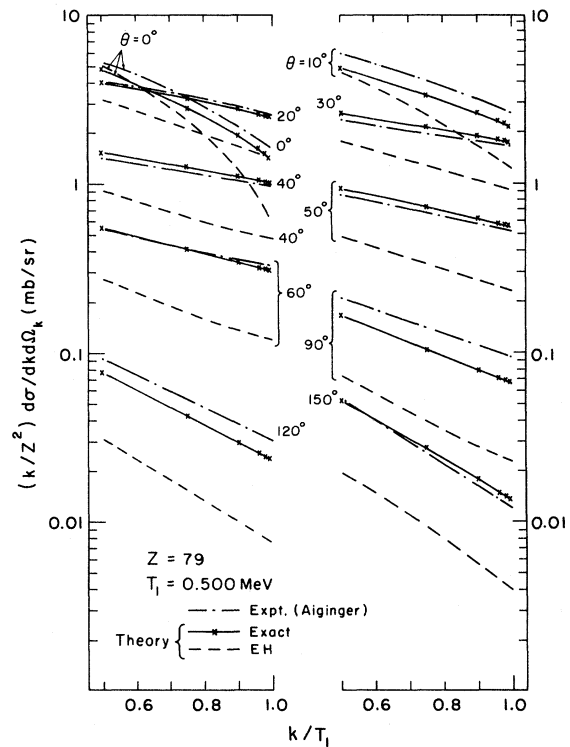


FIG. 2. Comparisons of the bremsstrahlung angular cross section $(k/Z^2) d\sigma/dk d\Omega_k$ for $Z=79$, $T_1=0.5$ MeV, $k/T_1=0.5-1.0$, $\theta=0^\circ-150^\circ$ between experimental data of Aiginger, our exact results, and results using EH formula.

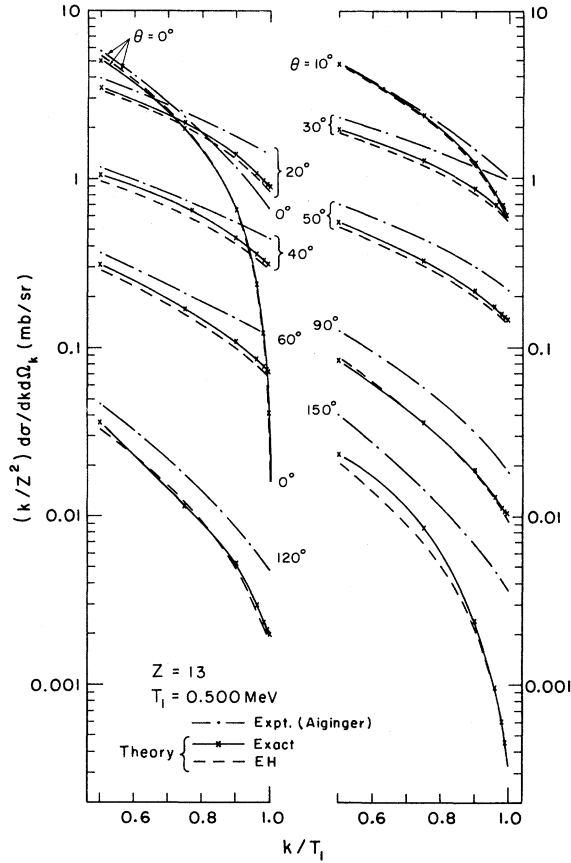


FIG. 3. Same as Fig. 2, except that $Z=13$.

More recently there have been relativistic point-Coulomb calculations of the bremsstrahlung matrix element using Sommerfeld-Maue (SM) wave functions. Bethe and Maximon¹¹ showed that SM wave functions will give exact results for bremsstrahlung in the limit of very high energies (supposed to mean 50 MeV, maybe as low as 15 MeV); they obtained the cross section assuming an initial high-energy electron and a final high-energy electron and high-energy photon emerging at very small angles relative to the incident direction. However, the SM wave function can also be obtained from the exact point-Coulomb wave function in partial waves by neglecting terms of order $(Z\alpha)^2$ relative to $(j + \frac{1}{2})^2$ in each partial wave, which corresponds to the neglect of terms of order $(Z\alpha)^2 / (j + \frac{1}{2})$ in the wave function. It is thus exact up to order $(Z\alpha)^2$ at all energies, and to this order it reduces to the exact nonrelativistic wave function at low energies. For these reasons EH calculated bremsstrahlung with SM wave functions without making the high-energy and small-angle assumptions of Bethe and Maximon. Their result reduces to the Sommerfeld formula at low energies and to the Bethe-Maximon results at high energies; for

low- Z elements it should be good at all energies. However, for high- Z elements at the intermediate energies reported in this paper, the EH formula does not improve upon Bethe-Heitler modified by the Elwert factor. We should note that since SM wave functions represent an approximation in $Z\alpha$, not in $Z\alpha/\beta$, these calculations do not suffer from the failure of Born approximation in the tip region of the spectrum.

The results described so far are obtained for a point-Coulomb potential. Only in the case of Born approximation can the modifications resulting from a screened potential be obtained. The result is to multiply the matrix element by a form factor $F(\Delta) = \int \rho e^{i\vec{\Delta} \cdot \vec{r}} d^3r$, where ρ is the charge distribution responsible for the potential V and $\vec{\Delta} = \vec{p}_1 - \vec{p}_2 - \vec{k}$ is the momentum transfer to the atom. The review article of Koch and Motz¹² discusses the importance of screening according to this form-factor approach. Although derived in Born approximation, the same form factor has been applied to the other analytic point-Coulomb calculations; our numerical data suggest that when modified in this way the Elwert-Haug predictions are fairly satisfactory for screened atoms of low Z .

We have already described our program⁵⁻⁷ for the numerical calculation of bremsstrahlung in screened potentials in the range 5 keV to 2 MeV. This permits an assessment of the importance of screening and Coulomb effects beyond Born approximation and so serves to delineate the circumstances in which the simpler analytic calculations are useful. For the tip region it is evident from Tables I and II and Figs. 1-3 that, as expected, Born approximation is unsatisfactory, but when modified by the Elwert factor it gives fairly good results for low- Z but not high- Z elements. Screening is unimportant in the low- Z cases, but significantly decreases the high- Z tip cross sections, by amounts increasing from 5% at 500 keV to 20% at 50 keV. We will subsequently discuss these results further.

III. TIP REGION OF THE SPECTRUM

We should now discuss in more detail the special situation for the tip region of the bremsstrahlung spectrum and explain why the spectrum remains finite at the tip (or, more correctly, close to the tip). It is easy to understand why the Bethe-Heitler cross section vanishes in the limit $p_2 \rightarrow 0$. In this Born approximation the final electron is described as a plane wave $e^{i\vec{p}_2 \cdot \vec{r}}$ and a first correction; both terms remain finite as $p_2 \rightarrow 0$. The cross section $\sigma \propto p_2 |M|^2$, where the matrix element M exists and is finite in the limit, so that σ vanishes with p_2 . By contrast, the exact point-Coulomb wave func-

tion does not remain finite in the limit, but for fixed r diverges as $p_2^{-1/2}$, thus leading to a cross section which remains finite. For example, for fixed r and small p_2 , the point-Coulomb continuum relativistic partial-wave components g_κ and f_κ become

$$g_\kappa = \eta_\kappa (\pi/2 p_2 Z \alpha)^{1/2} \left[\frac{1}{2} \rho J_{2\gamma-1}(\rho) - (\kappa + \gamma) J_{2\gamma}(\rho) \right], \quad (3)$$

$$f_\kappa = -\eta_\kappa (\pi Z \alpha / 2 p_2)^{1/2} J_{2\gamma}(\rho),$$

where

$$\rho = 2(2Z\alpha r)^{1/2}, \quad \gamma = (\kappa^2 - Z^2\alpha^2)^{1/2},$$

$$\eta_\kappa = -\kappa/|\kappa|.$$

These expressions were the basis for a numerical calculation of the point-Coulomb tip limit by Brysk, Zerby, and Penny.¹³ As we have already remarked, this difference corresponds to replacing the continuum normalization factor $N \propto |\nu / (1 - e^{-2\pi\nu})|^{1/2} \sim \nu^{1/2} \alpha p^{-1/2}$ for small p by the Born approximation (small- ν) value $N \propto (2\pi)^{-1/2}$. The Elwert factor uses the full N and so gives a finite tip cross section, as does the EH formula. The divergence of the exact wave function for small p is a consequence of the long-range nature of the point-Coulomb potential; it may be verified that if the potential is cut off at some distance the wave function then remains finite as $p \rightarrow 0$. Thus for the more realistic case of a screened potential we will again expect, as in the Born approximation, that the spectrum will vanish in the tip limit. If, however, for such a potential one asks how small p must be before one sees constant rather than $p^{-1/2}$ behavior, numerical calculations indicate that this requires a kinetic energy below ~ 100 eV. The calculations of this paper, for incident electrons of more than 5 keV, do not contemplate such fine energy resolution, and so for our present purposes we proceed as though the tip of the spectrum remains finite. The point-Coulomb tip spectrum point in the limit of very high T_1 was obtained by Jabbur and Pratt.¹⁴

For the incident electron energies considered here the important region of configuration space in the integral for the bremsstrahlung tip matrix element is at electron Compton wavelength distances.¹⁵ At or near the tip the momentum transfer Δ to the atom is $p_1 - k$. Energy conservation requires $(1 + p_1^2)^{1/2} = 1 + k$ (in units $\hbar = m_e = c = 1$), resulting in a *minimum* possible momentum transfer,

$$p_1 - k = 1 + p_1 - (1 + p_1^2)^{1/2}. \quad (4)$$

This is always positive (unlike photoeffect) and gradually decreases from 1 at high energies, remaining 0(1) until $T_1 \sim 10$ keV; by 2.5 keV Δ_{\min} has dropped to 0.1. When the minimum momentum

transfer is 0(1) we can expect that the integral for the matrix element will be cut off at Compton wave length distances. At such distances, well inside the atom, screened continuum wave functions will have a point-Coulomb shape; the only effect of screening is to modify their normalization. Numerical calculations indicate that the screening modification of an s -wave normalization only becomes substantial below 100 eV, while for higher partial waves the modification is increasingly large, even at 100 keV, though diminishing with increasing energy. At 1 keV and above the p -wave modification is only a few percent, but for d waves, etc., the change is substantial. We will discuss below (see Table III) that at these energies the s wave of the low-energy outgoing-electron wave function gives the dominant contribution, with a substantial contribution also from the p waves in high- Z elements. With these ideas one can understand how the tip cross section depends on electron screening. Thus for $Z=79$ screening effects drop from 15% at $T_1 = 50$ keV to 6% at $T_1 = 500$ keV, both because the relative importance of the low-energy p states (with a 12% screening effect in N^2) is decreasing and because the screening effects on the initial state are substantially less at the higher energy. For given T_1 in these cases the tip-region screening is relatively independent of k/T_1 (at 50 keV ranging from 17% to 15% as k/T_1 varies from 0.8 to 1.0) because the screening dependence of the low-energy p wave changes slowly with energy.

It was first noted by Fano³ that there is an approximate connection between tip bremsstrahlung and atomic photoeffect; the relationship between the processes has been discussed by Pratt.^{14,15} The connection arises because except at low energies (below 10 keV) both processes are characterized by Compton wavelength distances, and at such distances the shape of low-energy continuum and bound-state wave functions of given angular momentum are the same, independent of energy. As a result, except for normalization, reduced radial matrix elements for tip bremsstrahlung are complex conjugate to those for photoeffect. The cross section for tip-region bremsstrahlung with a final continuum s -wave electron can be related to the K (or L_I or M_I , etc.) photoeffect cross section, that for a final continuum p -wave to $2p$ photoeffect, etc. The connection can be made in each partial-wave, neglecting terms of relative order $(Z\alpha)^2$. In this approximation the total cross section for tip bremsstrahlung can be written as an appropriately weighted sum of photoeffect cross sections:

$$\frac{d\sigma}{dk} \Big|_{k/T_1=1} = \frac{T_1}{T_1 + 2} \sum_{j,l} R^2(n, l) \sigma_{\text{photo}}(n, l), \quad (5)$$

TABLE III. Comparisons of percentage contributions to the tip (or near tip) bremsstrahlung cross sections (k/Z^2) $d\sigma/dk$ for $Z=79$ from the s , p , d , and f states of the final electron according to the exact results for $T_1=0.05-1.84$ MeV, the extremely-high-energy work of Pratt, the extremely-high-energy work of Jabbur and Pratt (JP), and the results from the photoeffect-tip bremsstrahlung connections using exact K - (or L_{I-}), L_{II-} , and L_{III-} subshell photoelectric cross sections (photo-bremsstrahlung connection). Symbols Coul and KS refer to point-Coulomb and Kohn-Sham potentials, respectively.

Theory	Exact		Pratt		JP		Photo-bremsstrahlung connection				
T_1 (MeV)	0.050	0.050	0.050	0.180	0.500	1.84	∞	∞	0.050	0.180	0.500
k/T_1	0.98	0.98	0.99	0.98	0.99	0.99	1.0	1.0	1.0	1.0	1.0
Potential	Coul	KS	KS	KS	KS	KS	Coul	Coul	Coul	Coul	Coul
lj	$\sigma_{lj}/\sigma_{\text{total}} (\%)$										
$s_{1/2}$	30.3	34.2	34.5	53.6	63.6	65.3	66.1	64.0	31.7	53.2	61.6
$p_{1/2}$	20.1	22.5	22.6	20.9	18.8	18.4	18.8	20.9	31.3	24.9	22.4
$p_{3/2}$	28.3	31.1	31.2	21.5	15.7	14.0	15.1	13.6	37.0	21.9	16.0
$d_{3/2}$	7.9	5.3	5.1	1.9	0.9	0.9	...	0.7
$d_{5/2}$	9.4	6.3	6.1	2.0	1.0	1.2	...	0.8
$f_{5/2}$	1.6	0.3	0.2	0.08	0.03	0.04
$f_{7/2}$	1.9	0.3	0.2	0.08	0.03	0.07

where

$$R(n, l) = (Z\alpha)^{-1} n^{2+l} \left(\frac{(n+l)!}{(n-l-1)!} \right)^{-1/2}. \quad (6)$$

Note there is no sum over principal quantum n ; for each (j, l) we may take *any* convenient n , as the product $R^2\sigma$ is independent of n in this approximation. With this choice of normalization factors screening effects are neglected. Predictions for bremsstrahlung tip obtained in this way from photoeffect cross sections¹⁶ are shown in Table II; they are generally within 20% even for high- Z elements and T_1 as low as 50 keV. The relative contribution of various low-energy continuum partial waves to the cross section is shown in Table III. It had been known that for high energies the s -wave contribution is dominant, but that in high- Z elements the p -wave contribution is significant. The table shows that as T_1 decreases the importance of higher waves *increases*. This is very well predicted from the photoeffect connection results, which are also shown in Table III.

Let us now finally return to the comparison of our numerical calculations with the experimental results of SAU, shown in Figs. 1-3. Data are shown in Fig. 1 as a function of Z for the tip limit of the spectrum in the cases of photons radiated at 10° from incident electrons of kinetic energy 1.84 MeV. For medium- and high- Z elements agreement between the experiments and our calculations is fairly good, showing that the discrepancy between theory and experiment found by SAU was mainly due to the use of inaccurate theo-

retical approximations. However, for low- Z elements we agree with previous theory and disagree with experiment. One possible explanation is that the discrepancies reflect the existence of another process, electron-electron bremsstrahlung, which has not been explicitly included in the theoretical calculations. The relative importance of this process could be expected to increase as Z^{-1} , but since the kinematics of the experiment would exclude electron-electron bremsstrahlung if the atomic electrons were taken as free, it is difficult to estimate the magnitude of the process in this situation. It has also been pointed out to us that experiments with low- Z targets are especially sensitive to contaminants. For these reasons further experimental work to clarify the nature of this discrepancy would be very welcome. In Figs. 2 and 3 we show comparisons of the energy dependence of the bremsstrahlung spectrum near the tip for various photon angles and electrons of kinetic energy 500 keV incident on Au and Al, respectively. The agreement between the experimental data and our numerical results is good for high Z , as expected. However, the agreement for Al is poor in the tip region of the spectrum, improving as k/T_1 decreases and the expected cross section becomes larger.

ACKNOWLEDGMENTS

We wish to thank Dr. E. Haug for helpful discussions and Dr. H. Aiginger for communicating experimental results prior to publication.

*Supported in part by the National Science Foundation under Grant No. GP-32798.

†Present address: Department of Physics, National Central University, Chung-Li, Taiwan (Formosa), Republic of China.

¹B. Starek, H. Aiginger, and E. Unfried, *Phys. Lett.* **39A**, 151 (1972); H. Aiginger (private communication).

²H. A. Bethe and W. Heitler, *Proc. R. Soc. Lond.* **A146**, 83 (1934); F. Sauter, *Ann. Phys. (Leipz.)* **20**, 404 (1934); G. Racah, *Nuovo Cimento* **11**, 461 (1934); **11**, 467 (1934).

³U. Fano, *Phys. Rev.* **116**, 1156 (1959); K. W. McVoy and U. Fano, *ibid.* **116**, 1168 (1959); U. Fano, H. W. Koch, and J. W. Motz, *ibid.* **112**, 1679 (1958).

⁴G. Elwert and E. Haug, *Phys. Rev.* **183**, 90 (1969).

⁵H. K. Tseng and R. H. Pratt, *Phys. Rev. A* **1**, 528 (1970); **3**, 100 (1971).

⁶H. K. Tseng and R. H. Pratt, *Phys. Rev. A* **7**, 1502 (1973).

⁷H. K. Tseng and R. H. Pratt, *Phys. Rev. Lett.* **33**, 516

(1974).

⁸W. Kohn and L. S. Sham, *Phys. Rev.* **140**, A1133 (1965); D. A. Liberman, D. T. Cromer, and J. T. Waber, *Computer Phys. Commun.* **2**, 107 (1971).

⁹A. Sommerfeld, *Ann. Phys. (Leipz.)* **11**, 257 (1931).

¹⁰G. Elwert, *Ann. Phys. (Leipz.)* **34**, 178 (1939); E. Guth, *Phys. Rev.* **59**, 325 (1941).

¹¹H. A. Bethe and L. C. Maximon, *Phys. Rev.* **93**, 768 (1954).

¹²H. W. Koch and J. W. Motz, *Rev. Mod. Phys.* **31**, 920 (1959).

¹³H. Brysk, C. D. Zerby, and S. K. Penny, *Phys. Rev.* **180**, 104 (1969).

¹⁴R. J. Jabbur and R. H. Pratt, *Phys. Rev.* **129**, 184 (1963); **133**, B1090 (1964).

¹⁵R. H. Pratt, *Phys. Rev.* **120**, 1717 (1960); R. H. Pratt, A. Ron, and H. K. Tseng, *Rev. Mod. Phys.* **45**, 273 (1973).

¹⁶S. Hultberg, B. Nagel, and P. Olsson, *Ark. Fys.* **38**, 1 (1968); J. H. Scofield, Report No. UCRL-51326, Lawrence Livermore Laboratory, 1973 (unpublished).